

# 3D SIMULATION OF CONVECTION AND SPECTRAL LINE FORMATION IN A-TYPE STARS

M. Steffen<sup>1</sup>, B. Freytag<sup>2</sup>, and H.-G. Ludwig<sup>3</sup>

<sup>1</sup>Astrophysikalisches Institut Potsdam, An der Sternwarte 16, D-14482 Potsdam, Germany

<sup>2</sup>GRAAL, Université de Montpellier II, F-34095 Montpellier, France

<sup>3</sup>Lund Observatory, Box 43, S-22100 Lund, Sweden

## ABSTRACT

We present first realistic numerical simulations of 3D radiative convection in the surface layers of main sequence A-type stars with  $T_{\text{eff}} = 8000$  K and  $8500$  K,  $\log g = 4.4$  and  $4.0$ , recently performed with the CO<sup>5</sup>BOLD radiation hydrodynamics code. The resulting models are used to investigate the structure of the H+He I and the He II convection zones in comparison with the predictions of local and non-local convection theories, and to determine the amount of ‘overshoot’ into the stable layers below the He II convection zone. The simulations also predict how the topology of the photospheric granulation pattern changes from solar to A-type star convection. The influence of the photospheric temperature fluctuations and velocity fields on the shape of spectral lines is demonstrated by computing synthetic line profiles and line bisectors for some representative examples, allowing us to confront the 3D model results with observations.

Key words: Stars: A-type – Stars: convection – hydrodynamics – radiative transfer

## 1. INTRODUCTION

In comparison with the Sun, convection in the envelopes of A-type stars is a rather inefficient energy transport mechanism. According to local mixing-length theory (MLT, Böhm-Vitense 1958) convection is confined to two separate shallow convection zones near the stellar surface. Unfortunately, the structure and convective efficiency of these layers depends sensitively on the choice of the –unknown– mixing-length parameter. Another problem with MLT is that it cannot describe convective overshoot. To overcome these difficulties, ‘parameter-free’, non-local convection theories have been developed and applied to A-type stars (Kupka & Montgomery 2002, KM02).

Radiation hydrodynamics simulations of stellar convection constitute an independent approach. Up to now, *realistic* simulations of surface convection in A-type stars have been restricted to 2D (Freytag et al. 1996). 3D simulations are challenging, because the short radiative time scales in the atmospheres of these stars enforce an exceedingly small numerical time step, and hence make convection simulations for A-type stars much more time con-

suming than for the Sun. On the other hand, A-type stars have the advantage that the entire convective part of the envelope can be included in a single simulation box with a simple closed lower boundary.

In the following, we present first results of 3D hydrodynamical convection simulations for main-sequence A-type stars ( $T_{\text{eff}} = 8000$  K and  $8500$  K,  $\log g = 4.4$  and  $4.0$ , solar metallicity), and compare them with the aforementioned convection theories. We also address the interesting question of whether the hydrodynamical models can reproduce the peculiar line profiles and lines asymmetries (inverse bisector C-shape) observed for slowly rotating A-type stars with  $T_{\text{eff}}$  around  $8000$  K (Landstreet 1998).

## 2. 3D HYDRODYNAMICAL CONVECTION MODELS

The numerical simulations presented here were performed with CO<sup>5</sup>BOLD, a 3D radiation hydrodynamics code designed to model stellar convection (see Freytag et al. 2002 or Wedemeyer et al. 2004 for details). The integration of the equations of hydrodynamics is based on a conservative finite volume approach using an approximate Riemann solver of Roe type together with a *van Leer* reconstruction scheme. The Roe solver was modified to handle an external gravity field and an arbitrary tabulated equation of state (EOS). For the present application, we use a realistic EOS table accounting for partial ionization of hydrogen and helium (as well as H<sub>2</sub> molecule formation).

The 3D non-local radiative transfer is solved on a system of *long* rays, employing a modified Feautrier scheme. Using a realistic Phoenix-OPAL Rosseland mean opacity table, we adopt the grey approximation in this exploratory study. Strict LTE is assumed (no scattering), and radiation pressure is ignored.

The simulations are performed on a Cartesian grid with variable cell size in the vertical direction. We apply periodic lateral boundary conditions, while top and bottom boundaries are ‘closed’.

## 3. RESULTS

The results shown here are derived from convection simulations for stellar parameters  $T_{\text{eff}} = 8000$  K,  $\log g = 4.4$  (model 1), and  $T_{\text{eff}} = 8500$  K,  $\log g = 4.4$  (model 2), respectively. A representative snapshot from each of these sequences is displayed in Fig. 1. Similar calculations have

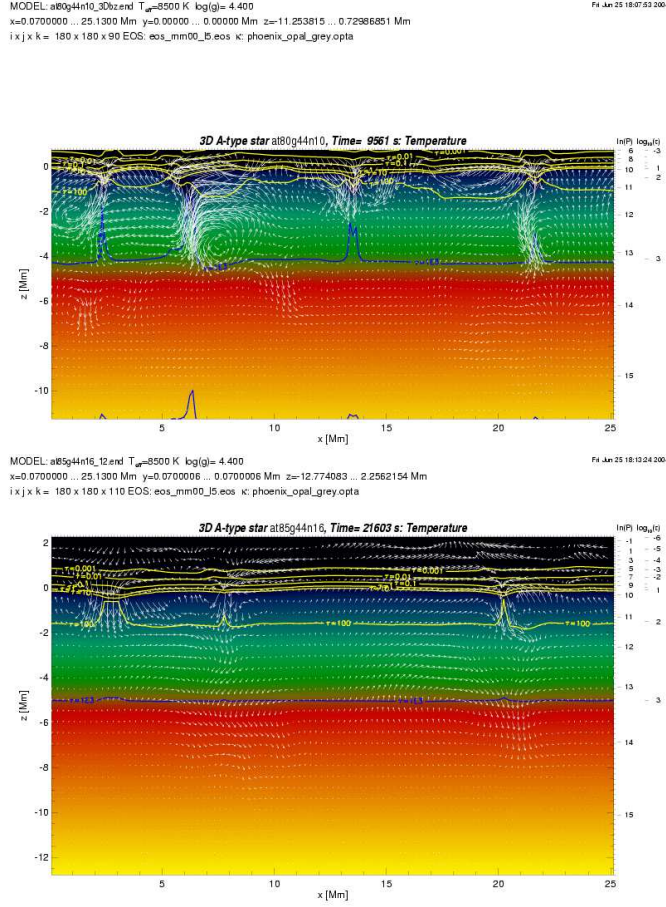


Figure 1. Arbitrary snapshots from two 3D simulations of convection in the surface layers of A-type stars, showing the velocity field and temperature distribution in a vertical slice. **Top:** MODEL 1:  $T_{\text{eff}} = 8000$  K,  $\log g = 4.4$ , geometrical size  $25.2 \times 25.2 \times 12.0$  Mm,  $180 \times 180 \times 90$  grid cells, vertical optical depth range  $-3 \leq \log \tau_{\text{Ross}} \leq 4$ , covering  $\approx 10$  pressure scale heights. **Bottom:** MODEL 2:  $T_{\text{eff}} = 8500$  K,  $\log g = 4.4$ , geometrical size  $25.2 \times 25.2 \times 15.0$  Mm,  $180 \times 180 \times 110$  grid cells,  $-6 \leq \log \tau_{\text{Ross}} \leq 4$ , covering  $\approx 16 H_p$ .

been performed for  $\log g = 4.0$ , but are not shown here. Further details can be found in Freytag & Steffen (2004).

### 3.1. VERTICAL STRUCTURE, COMPARISON WITH MLT

In Figs. 2 - 4, the mean vertical structure of the 3D hydrodynamical simulations, obtained by horizontal and temporal averaging, is compared with the results of standard MLT, in the version described by Mihalas (1978), for mixing length parameters  $\alpha=0.5$  and  $1.0$ . Clearly, *MLT does not even approximately match the hydrodynamical results*, no matter what value of  $\alpha$  is chosen. We note that the non-local convection models by Kupka & Montgomery (2002) are qualitatively more similar to the hydrodynamical solu-

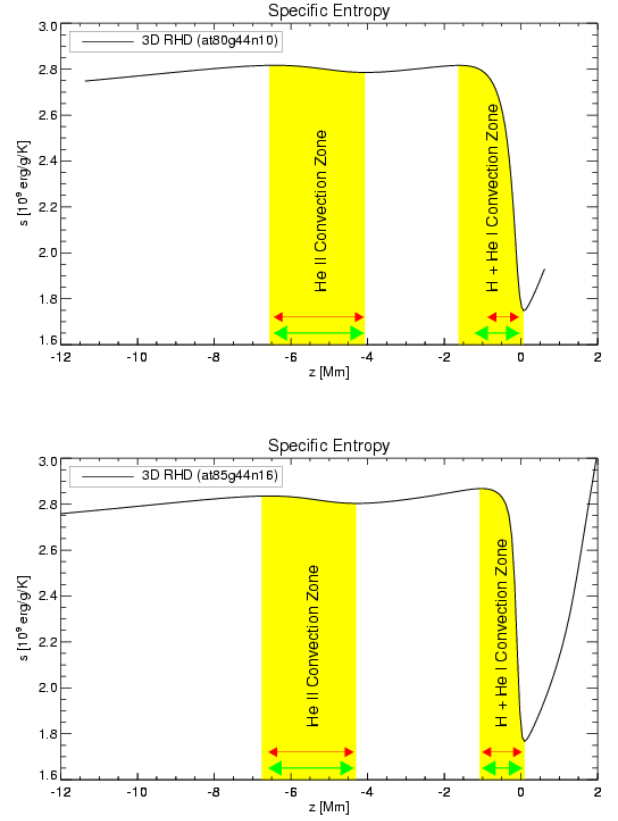


Figure 2. Mean specific entropy  $\langle s(z) \rangle_{x,y,t}$  for Model 1 (top) and Model 2 (bottom). In both cases, the entropy stratification indicates two separate convection zones ( $ds/dz < 0$ , shaded). The borders of convective instability according to local MLT models are indicated by thin ( $\alpha=0.5$ ) and thick ( $\alpha=1.0$ ) arrows.

tions, although considerable differences remain, especially in the energy fluxes. In contrast to the findings by KM02, our 3D models do not show anywhere a positive kinetic energy flux. Table 1 lists some key numbers characterizing the different kinds of models.

Fig. 4 demonstrates that ‘overshoot’ below the He II convection zone is substantial. The exponential tail of the velocity field is clearly seen in model 2, where the velocity scale height in terms of the pressure scale height at the bottom of the He II CZ is  $H_v/H_p \approx 0.4$ . Model 1 is not deep enough to include the exponential part of the overshoot region. We estimate  $H_v/H_p \lesssim 0.7$ .

### 3.2. HORIZONTAL STRUCTURE

The horizontal structure emerging from our 3D simulations of surface convection in A-type stars is evident from the intensity images displayed in Fig. 5. Obviously, the flow topology is qualitatively similar to that of the solar granulation, i.e. isolated hot up-flows (granules) are

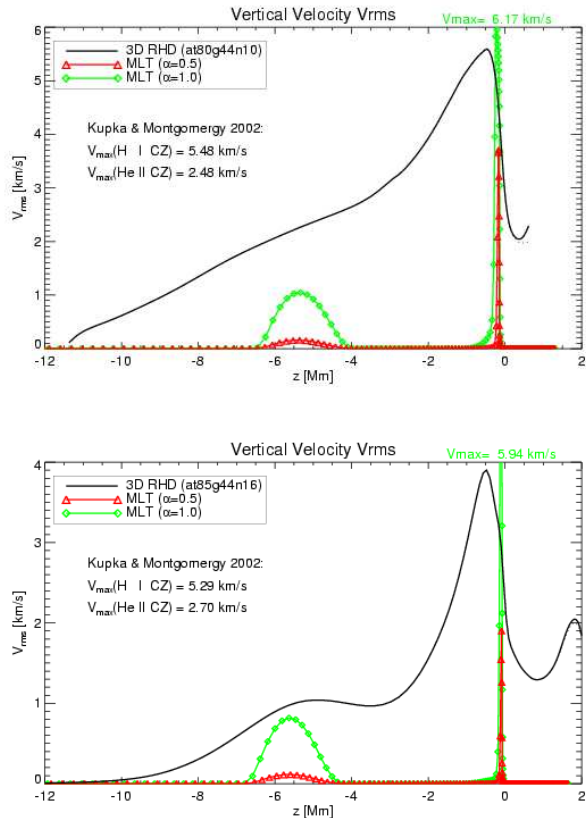


Figure 3. Mean vertical velocity  $\sqrt{\langle V_z^2(z) \rangle_{x,y,t}}$ , compared with MLT models. According to 3D hydrodynamics, both convection zones are connected by overshooting flows. The extended exponentially decaying flow field below the He II convection zone is also a result of ‘overshoot’.

separated by a network of connected cool down-flows (intergranular lanes). Due to a more efficient radiative energy exchange, the granules at the surface of A-type stars are relatively larger than on the Sun, and seem to show less sub-structure. In fact, the filling factor of dark areas (where  $I < \bar{I}$ ) is  $f_d \approx 0.34$  for both model 1 and model 2, compared to  $f_d \approx 0.53$  for the Sun.

### 3.3. SYNTHETIC LINE PROFILES

For the snapshots shown in Fig. 5, we have computed synthetic line profiles both for vertical rays (disk-center) and for integrated light (flux) under the assumption of LTE. The resulting disk-center line profiles and line bisectors of Fe I  $\lambda 6265.13 \text{ \AA}$  are presented in Fig. 6. The considerable photospheric velocities and temperature fluctuations induce a distinct asymmetry of the emergent line profiles. We have investigated several snapshots and different spectral lines, and found that the line bisector always exhibits a solar-like C-shape, but with a larger excursion to the red near the continuum. In the flux spectra, the line bi-

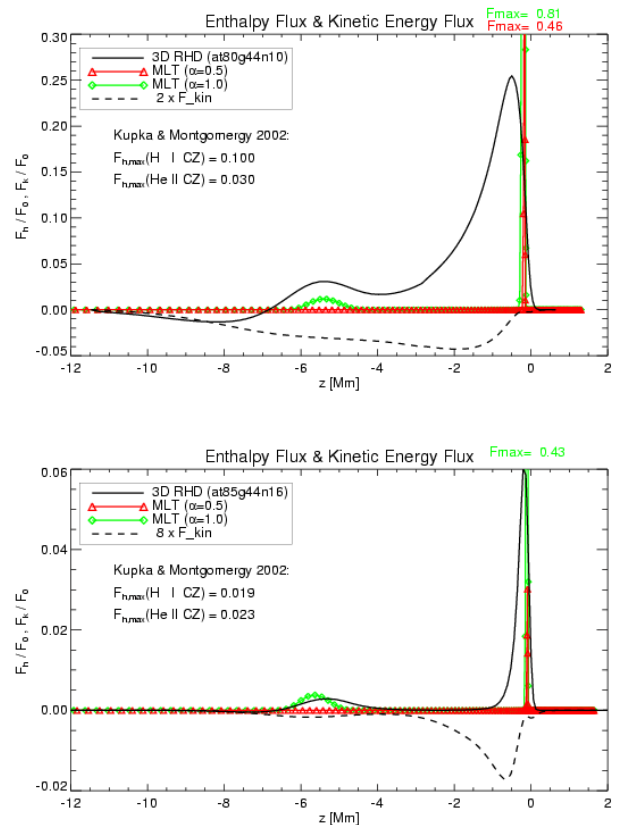


Figure 4. Mean enthalpy flux  $\langle \rho V_z h \rangle_{x,y,t}$ , compared with mixing-length results. Like in the solar granulation, the 3D simulations give a mean kinetic energy flux  $\langle \rho V_z V^2/2 \rangle_{x,y,t}$  which is directed downwards at all heights.

sectors span typically 2 km/s and 1 km/s for models 1 and 2, respectively. This is of the same order of magnitude as observed by Landstreet (1998), but the asymmetry is in the opposite direction. The C-shape persists for the simulations with  $\log g = 4.0$ .

### 4. CONCLUSIONS

The analysis of our 3D hydrodynamical simulations indicates a severe failure of the standard local mixing-length theory in the regime of A-type star shallow surface convection. The non-local convection model by Kupka & Montgomery (2002) gives a much better description of the velocity field, but alarming differences remain in the energy fluxes. Overshoot below the He II convection zone is found to be substantial, in basic agreement with KM02.

According to the simulations, the granulation pattern forming at the surface of A-type stars has a solar-like flow topology, with granules that are relatively larger than on the Sun and seem to show less sub-structure. Synthetic LTE line profiles based on the current 3D convection mod-

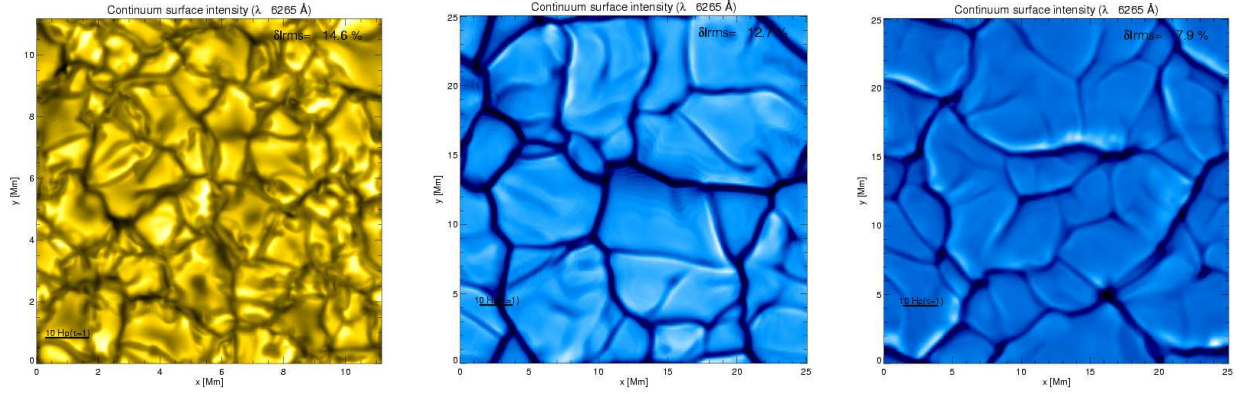


Figure 5. Emergent continuum intensity at  $\lambda 6265 \text{ \AA}$  resulting from 3D hydrodynamical simulations of the solar granulation (**left**,  $\delta I_{\text{rms}}=14.6\%$ ) and of surface convection in main-sequence A-type stars with  $T_{\text{eff}} = 8000 \text{ K}$  (**middle**,  $\delta I_{\text{rms}}=12.7\%$ ) and  $T_{\text{eff}} = 8500 \text{ K}$  (**right**,  $\delta I_{\text{rms}}=7.9\%$ ).

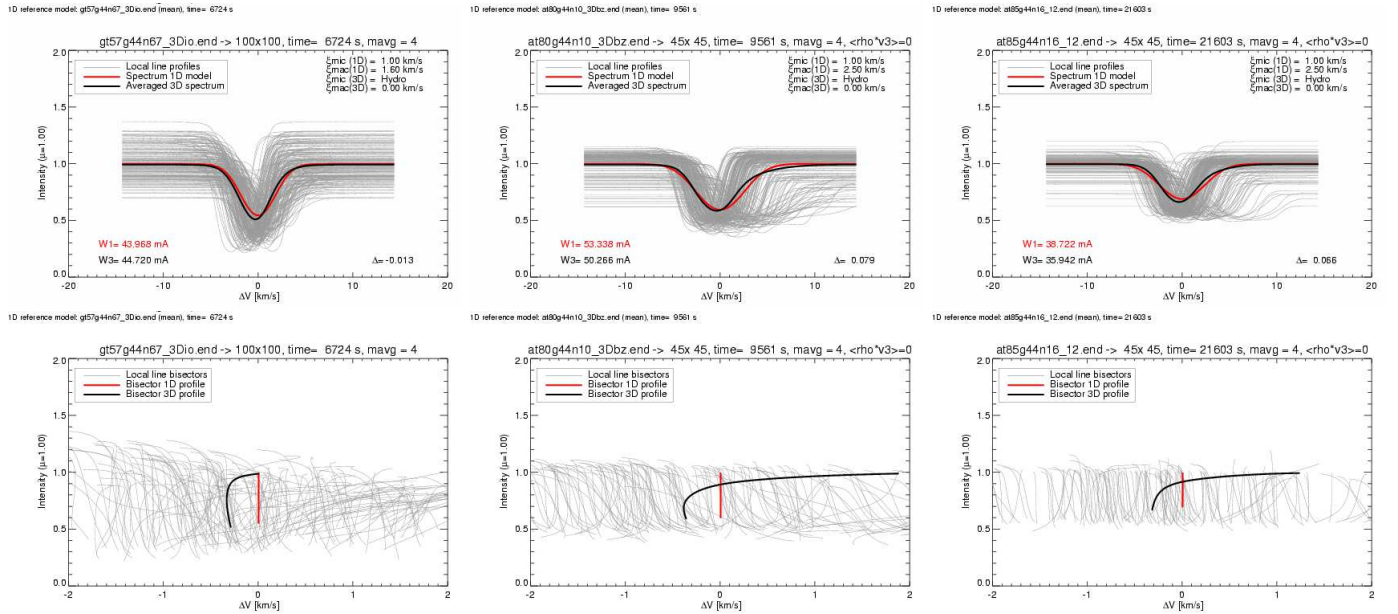


Figure 6. Spatially resolved and averaged line profiles (**top**) and line bisectors (**bottom**) of Fe I  $\lambda 6265.13 \text{ \AA}$ , computed from the snapshots shown in Fig. 5 for vertical lines-of-sight ( $\mu = 1$ ). For the Sun, the gf-value has been reduced by a factor 100. The asymmetry of the flux profiles (not shown) is qualitatively similar.

els of A-type stellar atmospheres show a depressed *red* wing, in apparent contradiction to the observed line asymmetry (Landstreet 1998). A possible reason for this discrepancy might be missing physics in the simulations (e.g. magnetic fields). On the other hand, we note that the slowly rotating A-type stars with  $T_{\text{eff}} \approx 8000 \text{ K}$  observed by Landstreet (1998) are classified as Am type and known to be spectroscopic binaries; hence they may be peculiar.

## REFERENCES

- Böhm-Vitense E. 1958, Z. Astrophys. 46, 108  
 Freytag B., Ludwig H.-G., Steffen M. 1996, A&A 313, 497  
 Freytag B., Steffen M., Dorch B. 2002, AN 323, 213

- Freytag B., Steffen M. 2004, in *The A-Star Puzzle*, J. Zverko, W.W. Weiss, J. Ziznovsky, S.J. Adelman, eds., IAU  
 Kupka F., Montgomery M.H. 2002, MNRAS 330, L6  
 Landstreet J.D. 1998, A&A 338, 1041  
 Mihalas D. 1978, *Stellar Atmospheres*, 2nd edition, Freeman  
 Wedemeyer S., Freytag B., Steffen M., Ludwig H.-G., Holweger H. 2004, A&A 414, 1121

Table 1. Comparison of maximum convective velocity,  $V_{c_{\max}}$  ([km/s]), maximum fraction of convective energy flux,  $F_{c_{\max}}$ , and of kinetic energy flux ( $Fk_{\max} \equiv \max(|Fk|)/F$ ) for different kinds of A-type star convection models. (u) and (l) refer to the upper (H+He I) and lower (He II) convection zone, respectively.

	Hydrodyn. Simulation	MLT $\alpha = 0.5$	MLT $\alpha = 1.0$	KM02 Theory
$T_{\text{eff}} = 8000 \text{ K}, \quad \log g = 4.40:$				
$V_{c_{\max}}(\text{u})$	5.59	3.71	6.17	5.48
$V_{c_{\max}}(\text{l})$	—	0.16	1.05	2.48
$F_{c_{\max}}(\text{u})$	0.255	0.458	0.806	0.100
$F_{c_{\max}}(\text{l})$	0.031	0.000	0.012	0.030
$Fk_{\max}(\text{u})$	0.0215	—	—	0.0011
$Fk_{\max}(\text{l})$	—	—	—	0.0012
$T_{\text{eff}} = 8500 \text{ K}, \quad \log g = 4.40:$				
$V_{c_{\max}}(\text{u})$	3.90	1.90	5.94	5.29
$V_{c_{\max}}(\text{l})$	1.04	0.11	0.82	2.70
$F_{c_{\max}}(\text{u})$	0.060	0.030	0.430	0.019
$F_{c_{\max}}(\text{l})$	0.003	0.000	0.004	0.023
$Fk_{\max}(\text{u})$	0.0021	—	—	0.0004
$Fk_{\max}(\text{l})$	0.0002	—	—	0.0010